Supplementary Information for

Representation of a two-way coupled irrigation system in the Common Land Model

Shulei Zhang[1, #], Hongbin Liang[1, #], Fang Li[2], Xingjie Lu[1], Yongjiu Dai[1]

[1] Southern Marine Science and Engineering Guangdong Laboratory (Zhuhai), School of Atmospheric Sciences, Sun Yat-sen University, Guangzhou, China

[2]International Center for Climate and Environment Sciences, Institute of Atmospheric Physics, Chinese Academy of Sciences, Beijing, 100029, China

Corresponding Author: Shulei Zhang (zhangshlei@mail.sysu.edu.cn) & Hongbin Liang (lianghb25@mail2.sysu.edu.cn)

[#] These authors contributed equally to this work.

1. Supplementary Figures

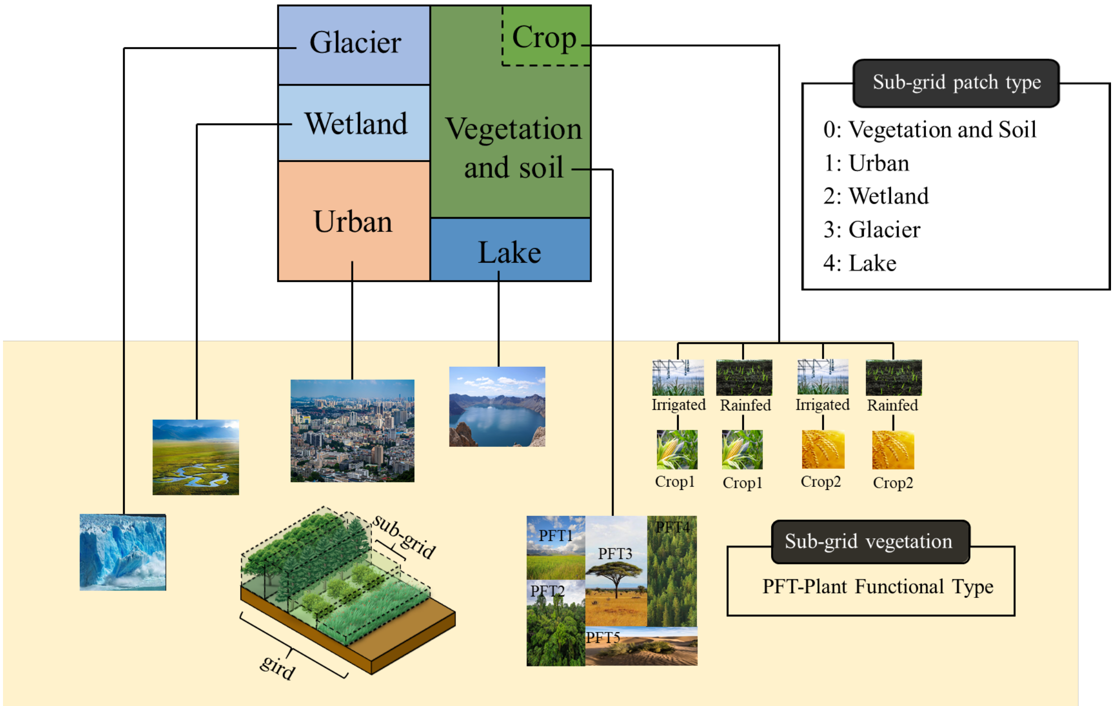

Figure S1. Diagram of the sub-grid structure in the Common Land Model.

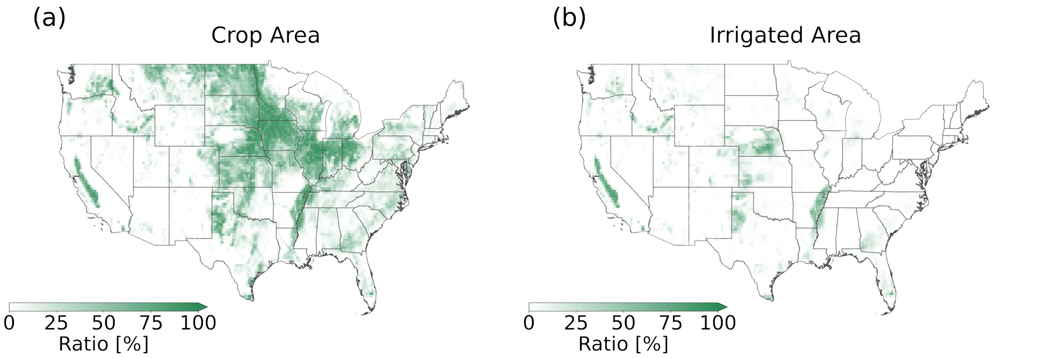

Figure S2. Spatial distribution of crop and irrigated area percentages within the study region. (a) Percentage of crop area. (b) Percentage of irrigated area.

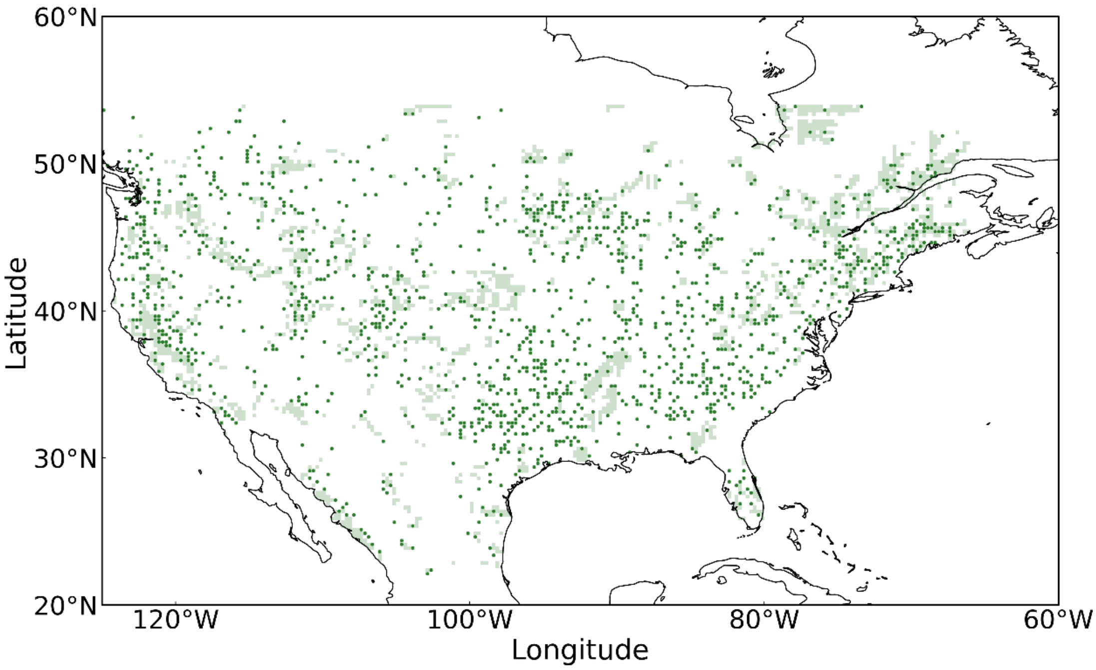

Figure S3. Locations of reservoirs and associated irrigated areas within the study region. Reservoir locations are marked with green dots, and the corresponding irrigated areas are shown in light green.

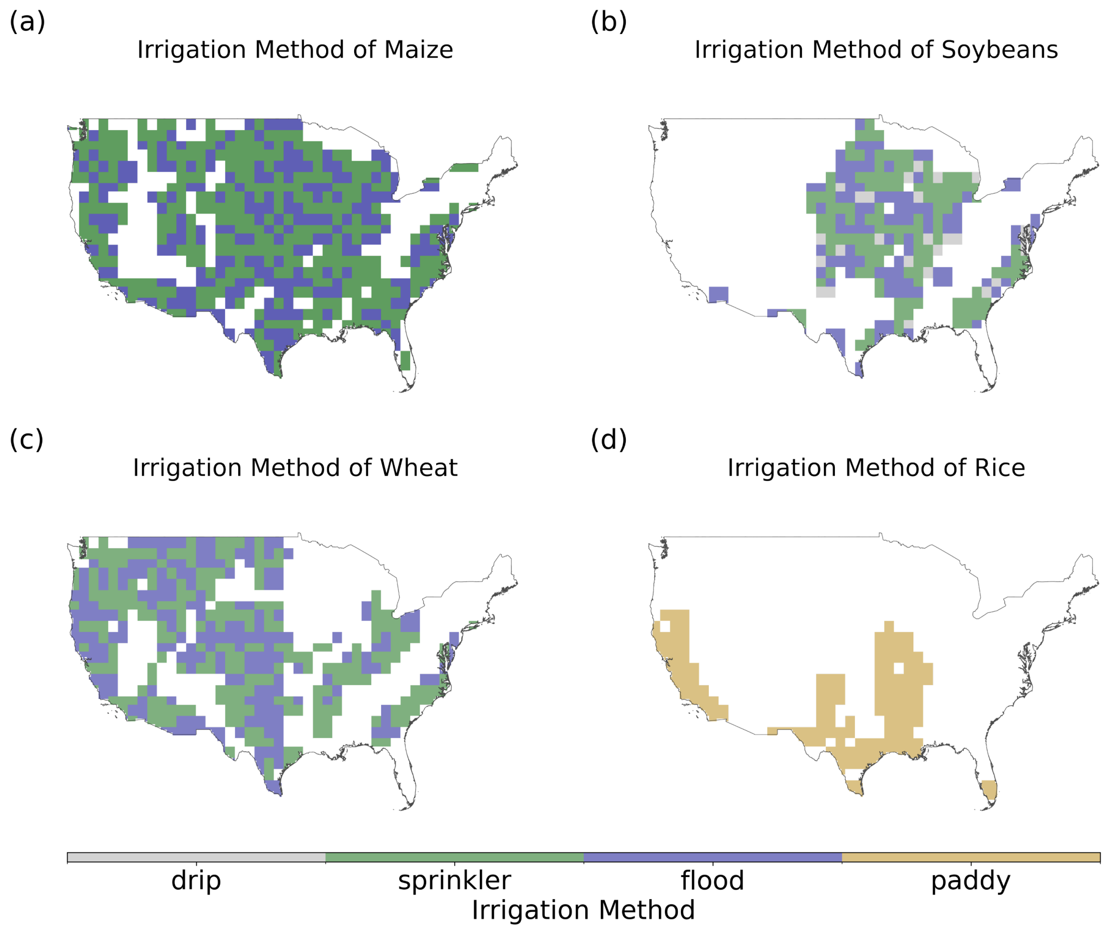

Figure S4. Irrigation methods for four crops across the study region. (a) Maize. (b) Soybeans. (c) Wheat. (d) Rice.

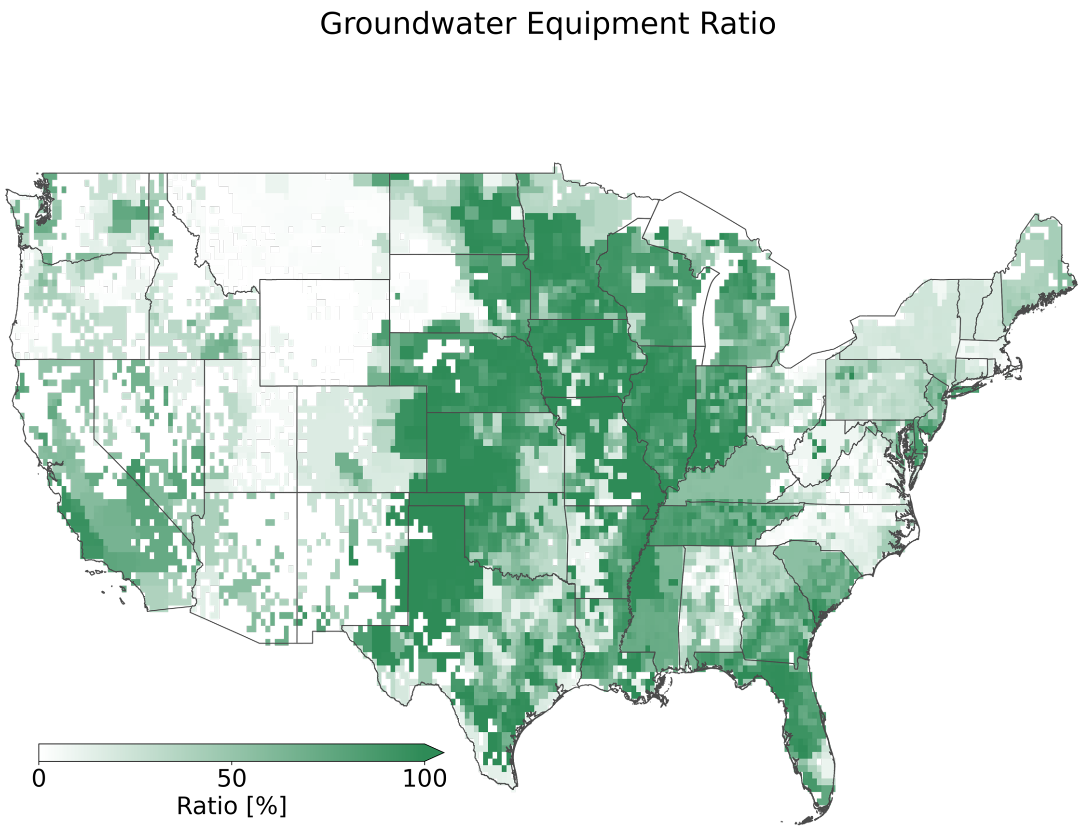

Figure S5. Percentage of area equipped with groundwater irrigation systems within the study region.

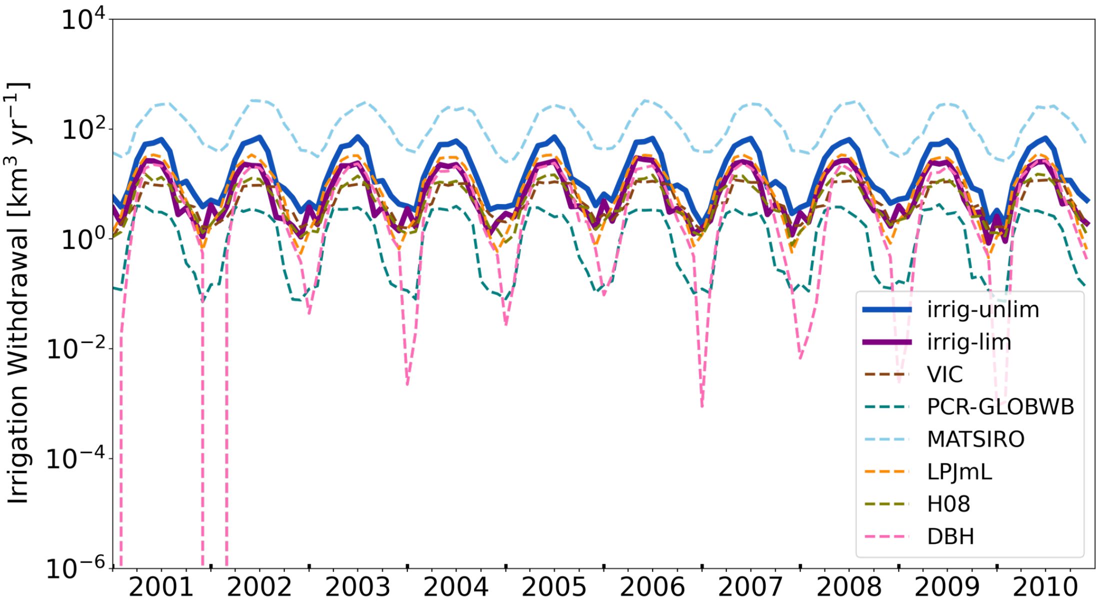

Figure S6. Time series of monthly total irrigation water withdrawal in the United States from 2001 to 2010, simulated by CoLM and the six global hydrological models participating in ISIMIP2a.

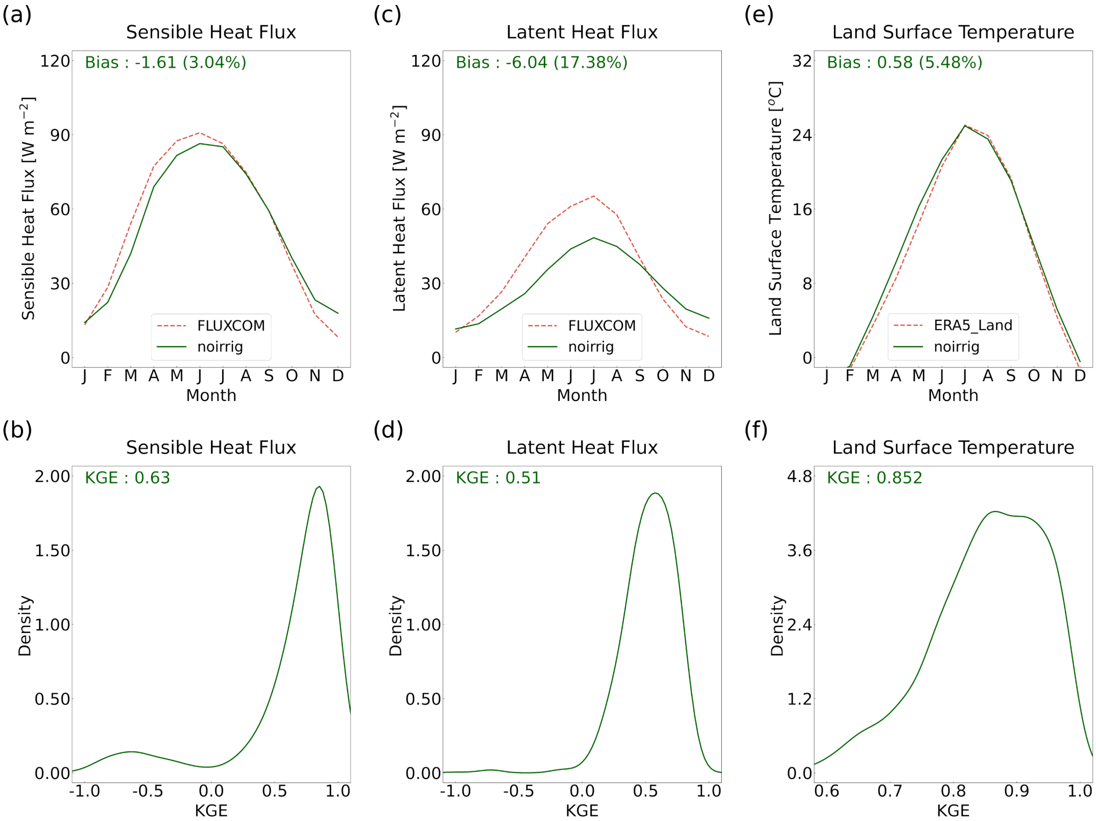

Figure S7. Evaluation of simulated energy fluxes and land surface temperature in the non-irrigation region. (a) Monthly sensible heat flux averaged from 2001 to 2016, based on the FLUXCOM dataset and simulated by CoLM using the noirrig scheme in non-irrigation regions of the United States, with the bias between simulations and observations (i.e., FLUXCOM) indicated in the panel. (b) Same as (a) but for latent heat flux. (c) Same as (a) but for land surface temperature, using data from ERA5-Land reanalysis dataset. (d) Kernel density estimate (KDE) curves for the Kling-Gupta efficiency (KGE) between observed and simulated monthly sensible heat flux for each non-irrigation grid, with mean KGE value indicated in the panel. (e-f) Same as (d) but for latent heat flux and land surface temperature.

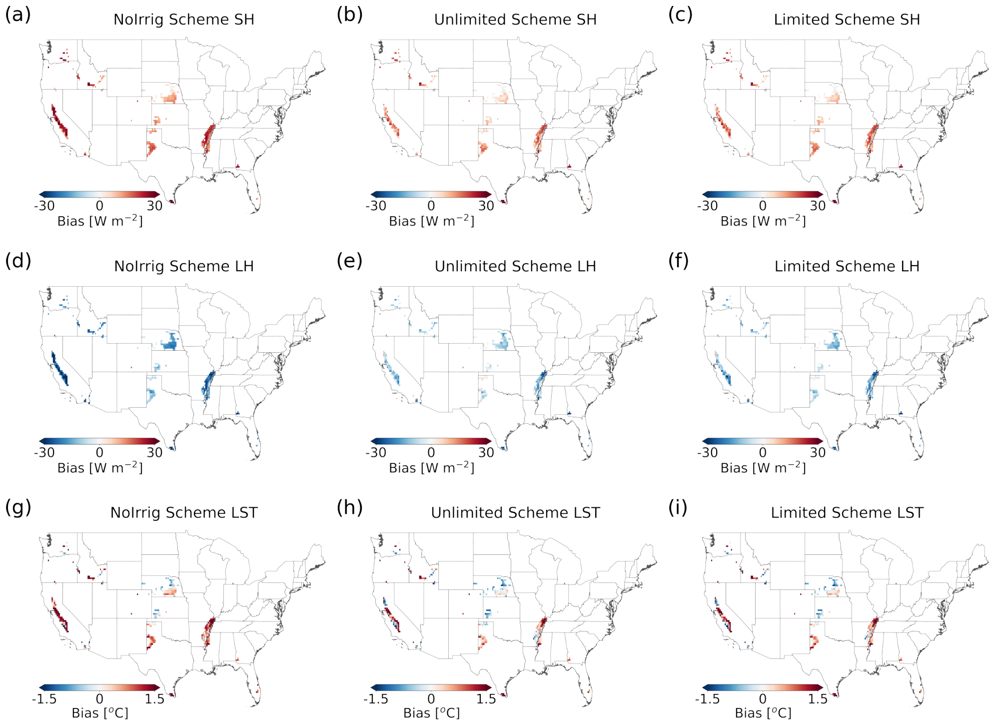

Figure S8. Evaluation of simulated energy fluxes and land surface temperature in the irrigation region. (a) Bias between observed monthly sensible heat flux and simulations from CoLM under the noirrig scheme in irrigation regions of the United States. (b) Same as (a) but for irrig-unlim scheme. (c) Same as (a) but for irrg-lim scheme. (d-f) Same as (a-c) but for latent heat flux. (g-i) Same as (a-c) but for or land surface temperature.

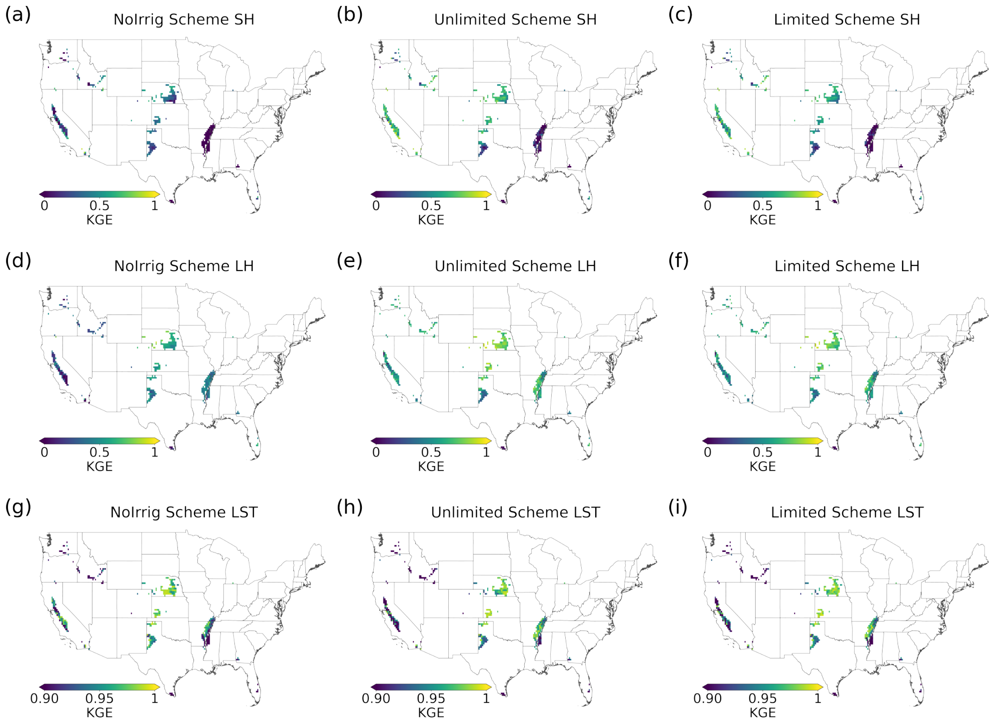

Figure S9. Evaluation of simulated energy fluxes and land surface temperature in the irrigation region. (a) The Kling-Gupta efficiency (KGE) between observed monthly sensible heat flux and simulations from CoLM under the noirrig scheme in irrigation regions of the United States. (b) Same as (a) but for irrig-unlim scheme. (c) Same as (a) but for irrg-lim scheme. (d-f) Same as (a-c) but for latent heat flux. (g-i) Same as (a-c) but for or land surface temperature.

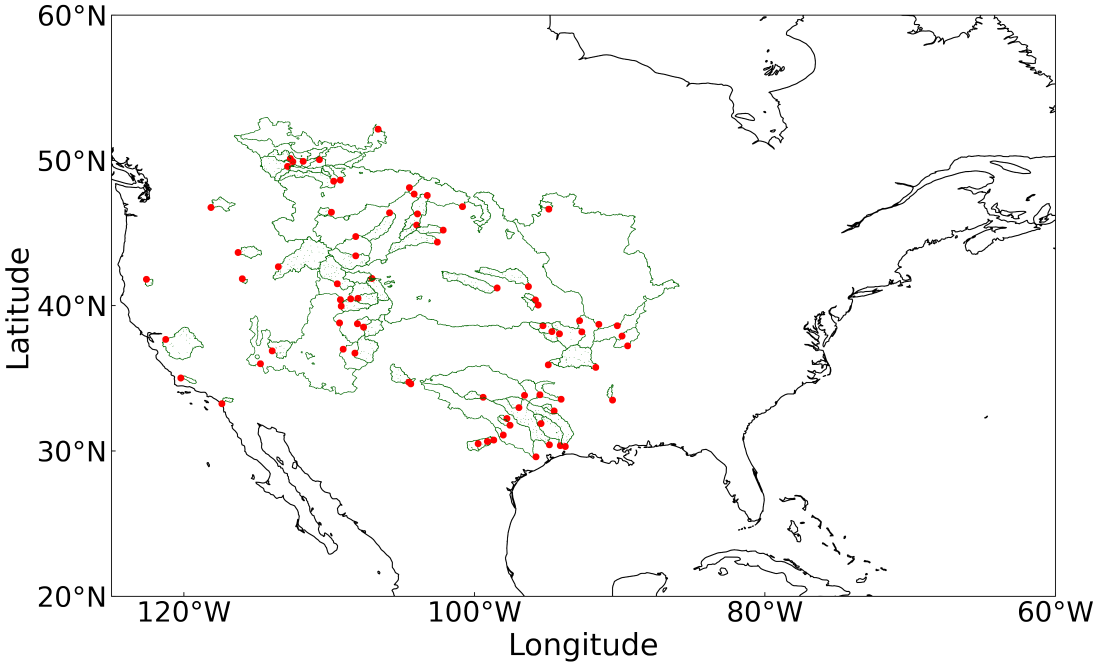

Figure S10. Locations of catchment outlets and boundaries of the 77 irrigation-affected catchments.

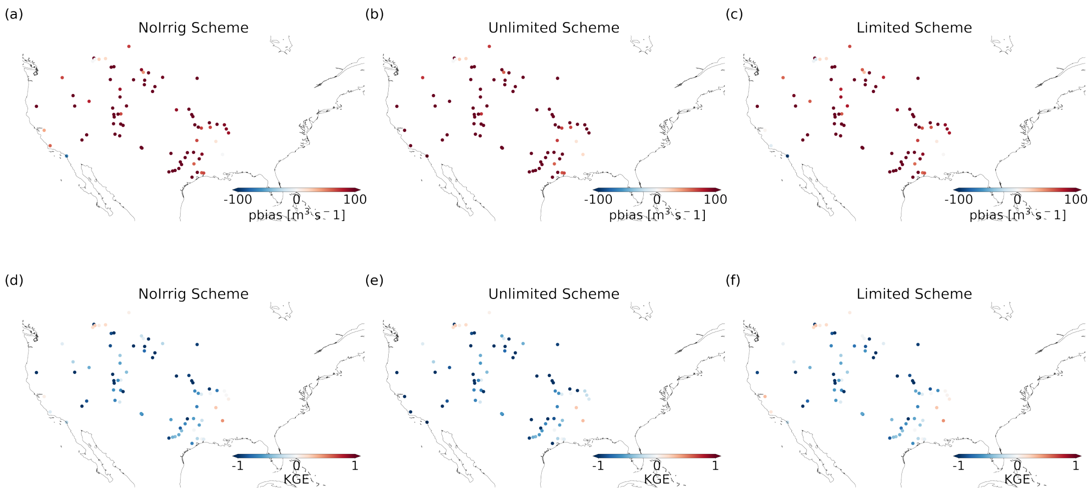

Figure S11. Evaluation of simulated streamflow in 77 irrigation-affected catchments. (a) Percentage bias (PBIAS) between observed monthly streamflow and simulations from CoLM under the noirrig scheme for each catchment. (b) Same as (a) but for irrig-unlim scheme. (c) Same as (a) but for irrg-lim scheme. (d-f) Same as (a-c) but for the Kling-Gupta efficiency (KGE) between simulated and observed streamflow.

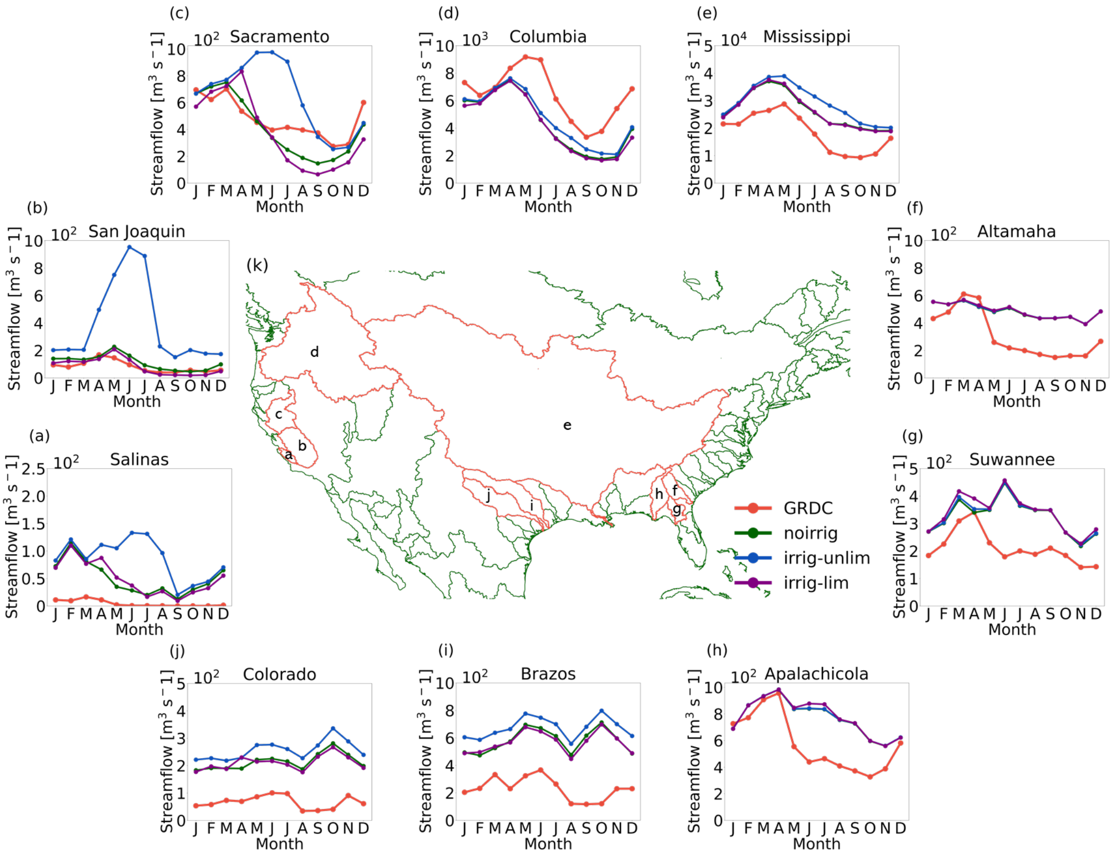

Figure S12. Evaluation of simulated streamflow in 10 large irrigation-affected catchments. (a-j) Monthly streamflow averaged from 2001 to 2016 for each catchment, based on GRDC dataset (red lines) and simulated by CoLM using the noirrig (green lines), irrig-unlim (blue lines), and irrig-lim schemes (purple lines). (k) Boundaries of the selected 10 irrigation-affected catchments (red lines).

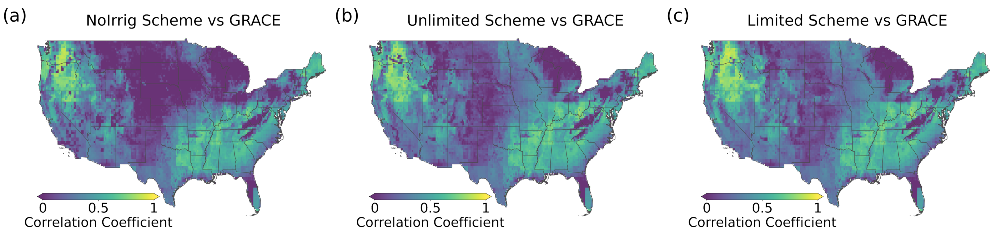

Figure S13. Comparison of observed and simulated monthly terrestrial water storage anomalies in the United States. (a) Spatial distribution of the Pearson correlation coefficient (r) between GRACE-derived TWS anomalies (JPL dataset) and CoLM simulations under the noirrig scheme. (b–c) Same as (a) but for the irrig-unlim and irrig-lim schemes, respectively.

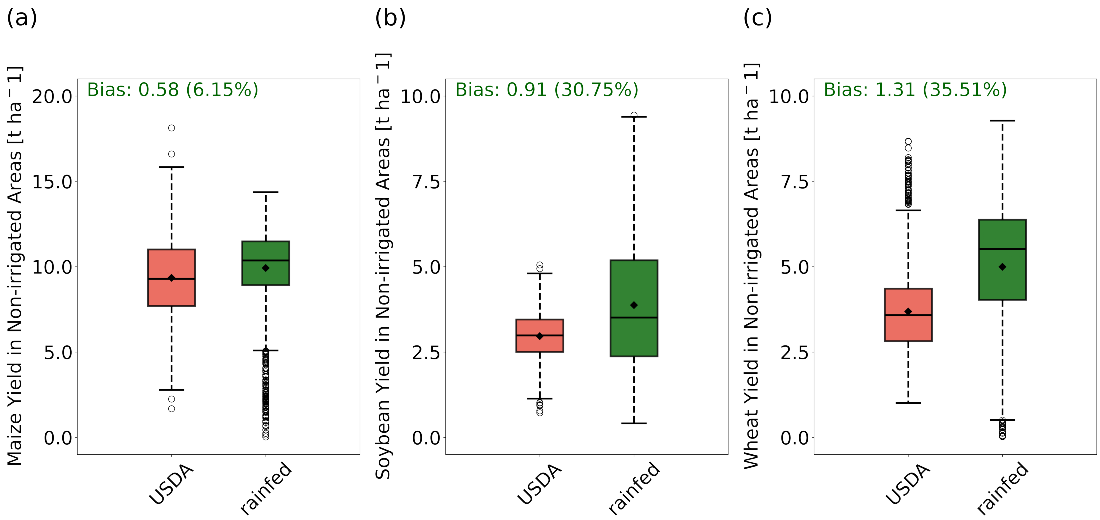

Figure S14. Evaluation of crop yield simulated in the United States. (a) Maize yield in rainfed maize-growing regions of the United States, as reported by the USDA (orange boxes), compared with simulations by CoLM in the non-irrigation region (green boxes). Since reported yields are at the county scale, grid-based simulation results were aggregated to corresponding counties. The boxes represent the interquartile range, black lines indicate median values, black dots show mean values, and dashed black whiskers extend to 1.5 times the interquartile range; points outside the boxes represent outliers. (b-c) Same as (a) but for soybean and wheat yields.

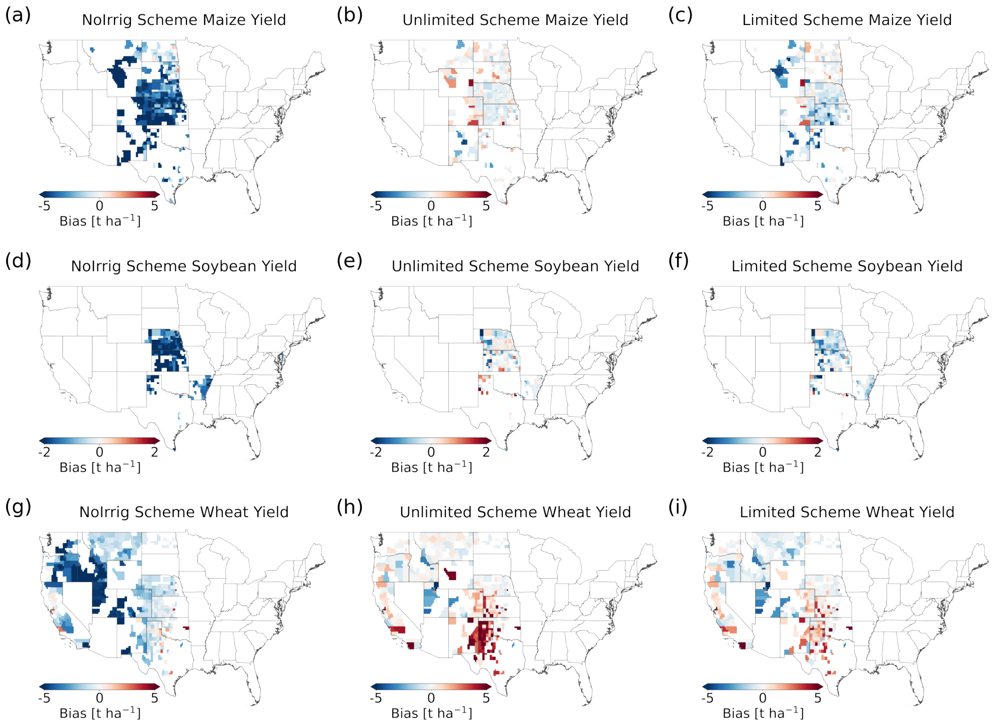

Figure S15. Evaluation of simulated crop yield in the irrigation region. (a) Bias between observed maize yield and simulations from CoLM under the noirrig scheme in irrigation regions of the United States. (b) Same as (a) but for irrig-unlim scheme. (c) Same as (a) but for irrg-lim scheme. (d-f) Same as (a-c) but for soybean yield. (g-i) Same as (a-c) but for or wheat yield.

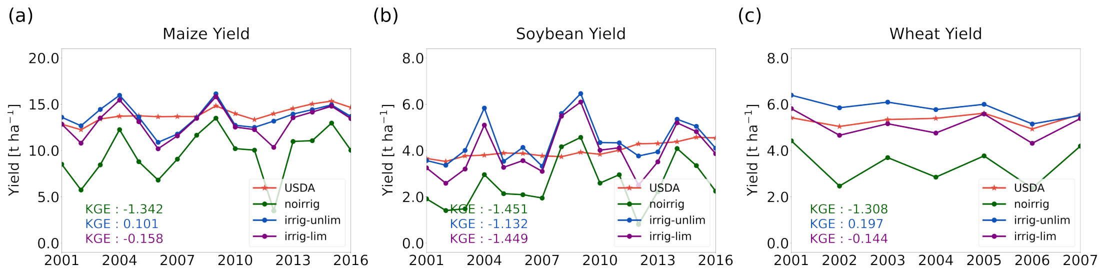

Figure S16. Comparison of observed and simulated annual yield variations for three crops in the United States. (a) Annual maize yield in irrigated maize-growing regions of the United States from 2001 to 2016, as reported by the USDA (orange lines), compared with simulations by CoLM using the noirrig (green lines), irrig-unlim (blue lines), and irrig-lim (purple lines) schemes. KGE values for the three simulation schemes are indicated in the panel. (b-c) Same as (a), but for annual soybean and wheat yields.

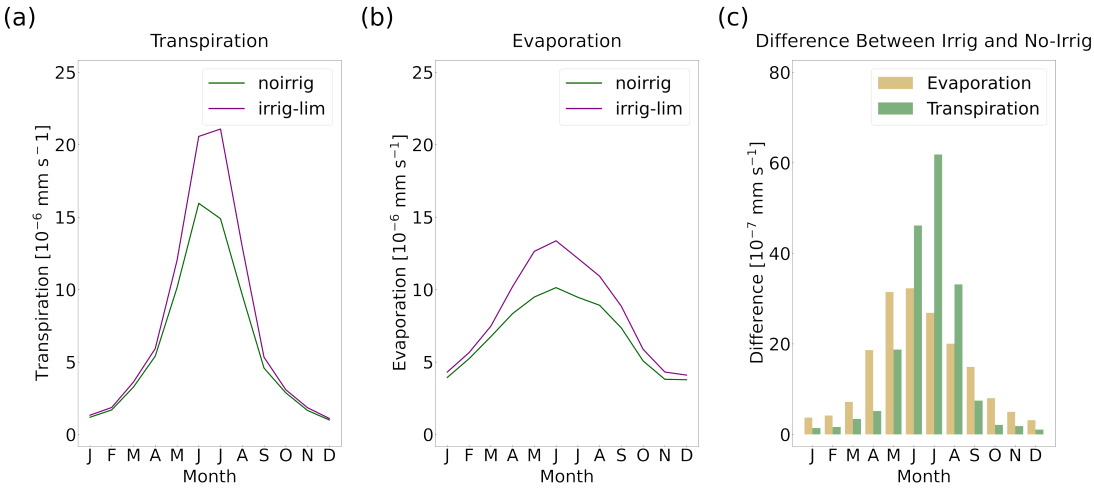

Figure S17. Differences in simulated evaporation and transpiration with and without irrigation. (a-b) Monthly transpiration (a) and evaporation (b) averaged from 2001 to 2016, simulated by CoLM using the noirrig and irrig-lim schemes in irrigation regions of the United States. (c) Monthly average differences in simulated transpiration and evaporation between the noirrig and irrig-lim schemes.

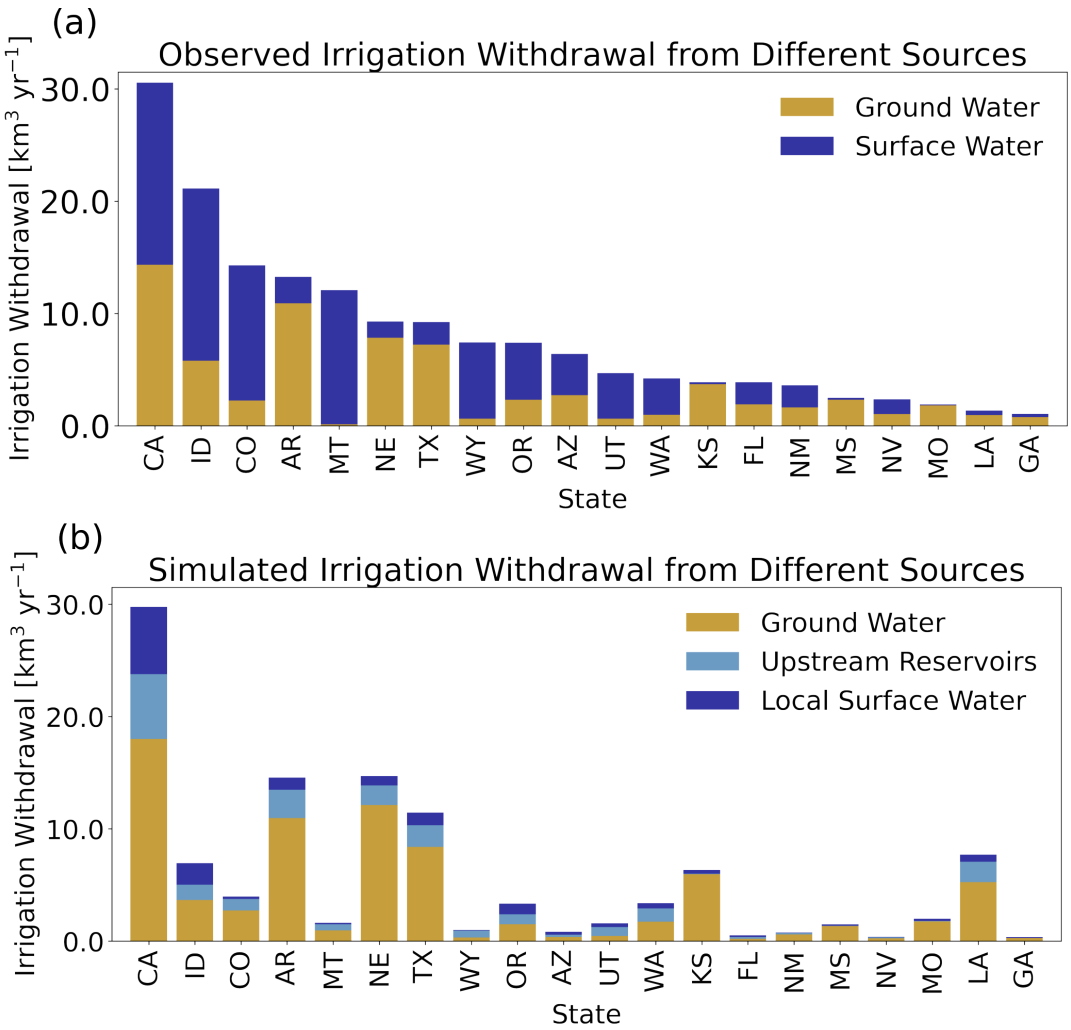

Figure S18. Comparison of reported and simulated annual irrigation water withdrawal by water source. (a) Annual withdrawal amounts from different sources for the top 20 states by irrigation water withdrawal, using data from USGS reports. (b) Same as (a), but for simulated by CoLM using the irrig-lim scheme.

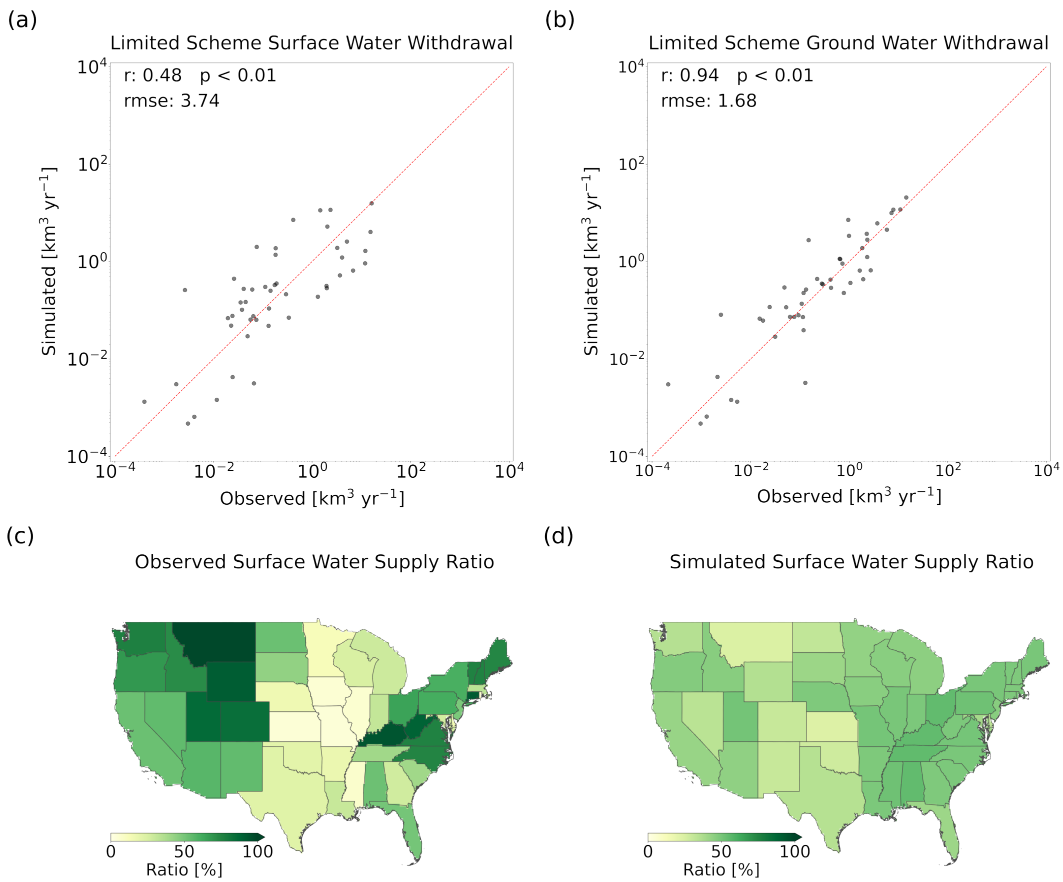

105
106 **Figure S19.** Comparison of reported and simulated irrigation water withdrawal in the United
107 States by water source using a sequential water withdrawal method. (a) Proportion of surface
108 water in irrigation withdrawal based on USGS reports for individual states. (b) Proportion of
109 surface water in irrigation withdrawal simulated by CoLM for individual states using the
110 sequential water withdrawal method. In this approach, water demand is not pre-allocated between
111 surface and groundwater sources but is met sequentially, with surface water withdrawn first,
112 followed by groundwater.

2. Supplementary Tables

Table S1. Key differences among various irrigation methods.

Feature	Drip	Sprinkler	Flood	Paddy
Irrigation trigger $\theta_{trigger}$	Φ_{sfc} *	Φ_{sfc}	Φ_{sfc} **	Φ_0
Irrigation target θ_{target}	Φ_{sfc}	Φ_{sfc}	Φ_0	Φ_0
Water application location	Surface	Above the canopy	Surface	Surface with ponding

* Φ_{sfc} represents field capacity, ** Φ_0 represents soil saturation.

Table S2. Total storage capacity and irrigation area of reservoirs of different scales (Ministry of Water Resources of China, 2017).

Engineering Grade	Reservoir Scale	Total Storage Capacity (billion m³)	Irrigation Area (100,000 mu)*
I	Large (Type 1)	> 10	> 150
II	Large (Type 2)	10 - 1	150 - 50
III	Medium	1 - 0.1	50 - 5
IV	Small (Type 1)	0.1 - 0.01	5 - 0.5
V	Small (Type 2)	0.01 - 0.001	< 0.5

* mu is a unit of area (1 mu ≈ 666.67 square meters).

Table S3. Observed and simulated irrigation water withdrawals ($km^3\ yr^{-1}$).

Sources	USGS	irrig-unlim	irrig-lim
Total	166.23	290.94	120.81
Surface	92.60	NA	37.78
Groundwater	73.63	NA	81.43

3. Supplementary Text

3.1 Evaluation of crop phenology

We selected multiple crop sites from FLUXNET and AmeriFlux, with details provided in the Table S4, including only stations where the same crop had been sown for more than two years. The results indicate that the model effectively captures the seasonal dynamics of LAI across different sites, regardless of whether the crops are rainfed or irrigated (Figures S20 and S21). However, LAI values were underestimated at certain site years, such as US-Ne3 in 2002 and 2006, when rainfed soybean was planted (Figure S20 (d and f)). The underestimation is primarily due to the proximity of US-Ne3 to irrigated sites (US-Ne1 and US-Ne2), where soil moisture conditions may be influenced by nearby irrigation. In contrast, the simulated LAI for rainfed soybean at US-IB1 closely aligns with observed values.

Table S4. Stations information.

station	location	LAI years	crop type	irrigation management
US-Ne1 (Suyker, 2024a)	41.18N, 96.44W	2002; 2004; 2006	maize	irrigated
US-Ne2 (Suyker, 2024b)	41.16N, 96.47W	2002, 2004, 2006	soybean	irrigated
US-Ne3 (Suyker, 2024c)	41.18N, 96.44W	2001, 2003, 2005	maize	rainfed
US-Ne3 (Suyker, 2024c)	41.18N, 96.44W	2002, 2004, 2006	soybean	rainfed
US-IB1 (Matamala, 2019)	41.86N, 88.22W	2005; 2007	soybean	rainfed
US-ARM (Biraud et al., 2024)	36.61N, 97.49W	2005; 2008	maize	rainfed
US-ARM (Biraud et al., 2024)	36.61N, 97.49W	2002; 2008	winter wheat	rainfed

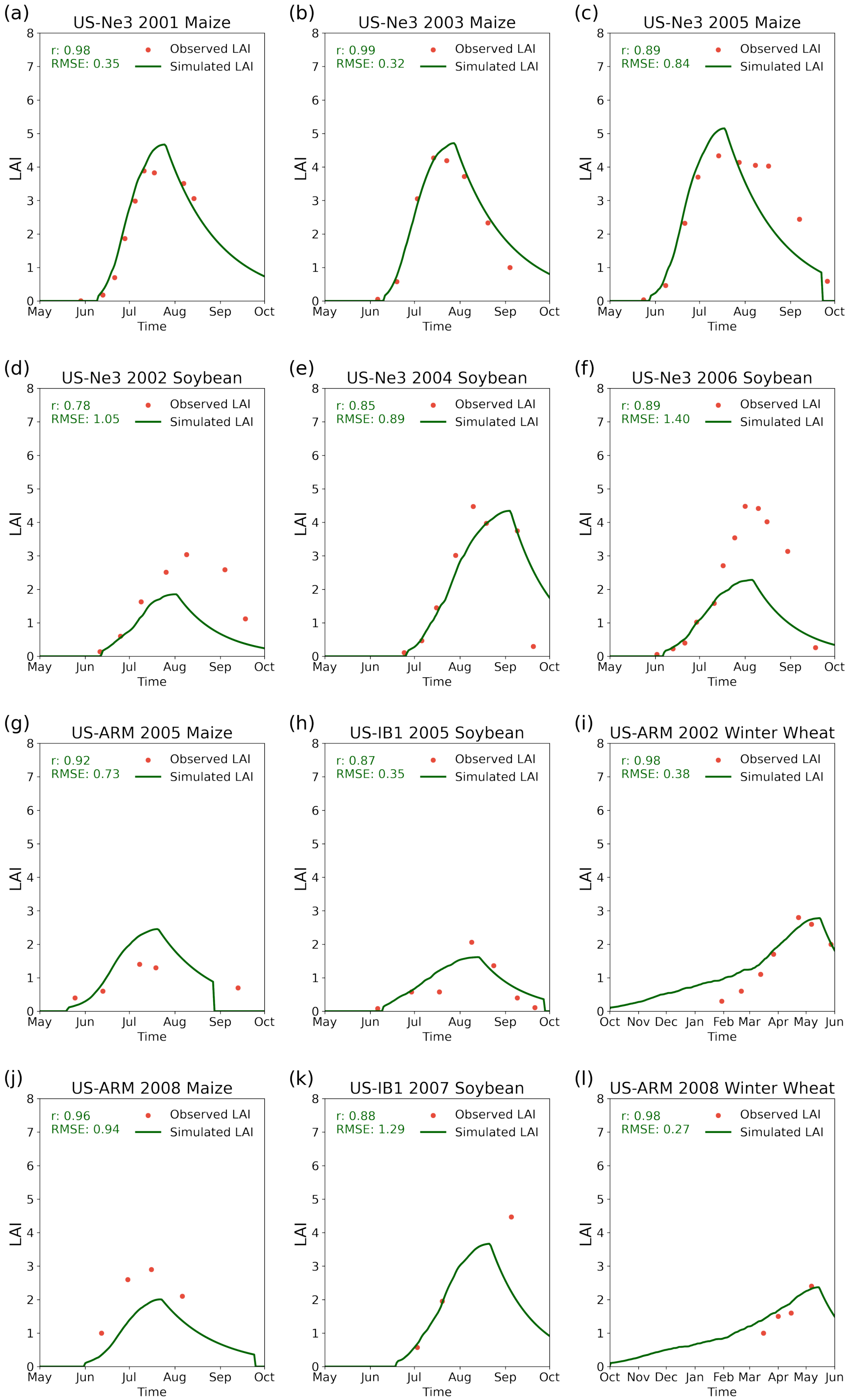
(a)
US-Ne3 2001 Maize
r: 0.98
RMSE: 0.35
(b)
US-Ne3 2003 Maize
r: 0.99
RMSE: 0.32
(c)
US-Ne3 2005 Maize
r: 0.89
RMSE: 0.84
(d)
US-Ne3 2002 Soybean
r: 0.78
RMSE: 1.05
(e)
US-Ne3 2004 Soybean
r: 0.85
RMSE: 0.89
(f)
US-Ne3 2006 Soybean
r: 0.89
RMSE: 1.40
(g)
US-ARM 2005 Maize
r: 0.92
RMSE: 0.73
(h)
US-IB1 2005 Soybean
r: 0.87
RMSE: 0.35
(i)
US-ARM 2002 Winter Wheat
r: 0.98
RMSE: 0.38
(j)
US-ARM 2008 Maize
r: 0.96
RMSE: 0.94
(k)
US-IB1 2007 Soybean
r: 0.88
RMSE: 1.29
(l)
US-ARM 2008 Winter Wheat
r: 0.98
RMSE: 0.27
Observed LAI
Simulated LAI
LAI
Time
May Jun Jul Aug Sep Oct
Oct Nov Dec Jan Feb Mar Apr May Jun

Figure S20. Comparison of reported and simulated LAI phenology at rainfed stations. (a) US-Ne3 for maize in 2001, as reported by the AmeriFlux (red dots), compared with simulations by CoLM without irrigation (green line). (b-c) Same as (a) but in 2003 and 2005. (d-f) Same as (a) but for soybean in 2002, 2004 and 2006. (g) and (j) Same as (a) but for maize at US-ARM in 2005 and 2008. (h) and (k) Same as (a) but for soybean at US-IB1 in 2005 and 2007. (i) and (l) Same as (a) but for winter wheat at US-ARM in 2002 and 2008.

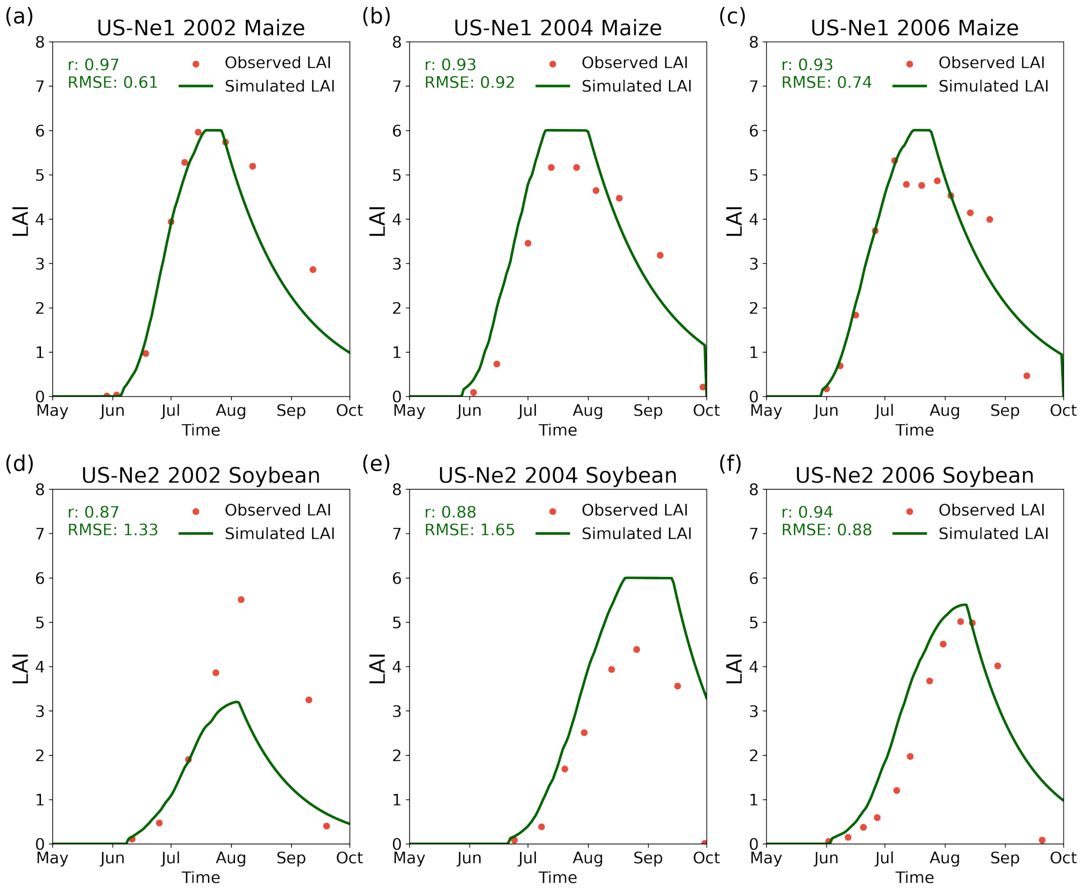

Figure S21. Comparison of observed and simulated LAI phenology at irrigated stations. (a-c) US-Ne1 for maize in 2002, 2004 and 2006, as reported by the AmeriFlux (red dots), compared with simulations by CoLM with irrigation (green line). (d-f) Same as (a-c) but for soybean at US-Ne2 in 2002, 2004 and 2006.

4. Supplementary References

Ministry of Water Resources of China: Standard for rank classification and flood protection criteria of water and hydropower projects, SL 252–2017, http://121.36.94.83:9008/jsp/yishenqing/appladd/biaozhunfile/detail.jsp?bzbh=SL%2B252-2017# (last access: October 2023), 2017

Suyker, A.: AmeriFlux BASE US-Ne1 Mead - irrigated continuous maize site, Ver. 18-5, AmeriFlux AMP, [Dataset], https://doi.org/10.17190/AMF/1246084, 2024a

Suyker, A.: AmeriFlux BASE US-Ne2 Mead - irrigated maize-soybean rotation site, Ver. 18-5, AmeriFlux AMP, [Dataset], https://doi.org/10.17190/AMF/1246085, 2024b

Suyker, A.: AmeriFlux BASE US-Ne3 Mead - rainfed maize-soybean rotation site, Ver. 18-5, AmeriFlux AMP, [Dataset], https://doi.org/10.17190/AMF/1246086, 2024c

Matamala, R.: AmeriFlux BASE US-IB1 Fermi National Accelerator Laboratory- Batavia (Agricultural site), Ver. 8-5, AmeriFlux AMP, [Dataset], https://doi.org/10.17190/AMF/1246065, 2019

Biraud, S., Fischer, M., Chan, S., and Torn, M.: AmeriFlux BASE US-ARM ARM Southern Great Plains site- Lamont, Ver. 13-5, AmeriFlux AMP, [Dataset], https://doi.org/10.17190/AMF/1246027, 2024